General Disclaimer

One or more of the Following Statements may affect this Document

- This document has been reproduced from the best copy furnished by the organizational source. It is being released in the interest of making available as much information as possible.

- This document may contain data, which exceeds the sheet parameters. It was furnished in this condition by the organizational source and is the best copy available.

- This document may contain tone-on-tone or color graphs, charts and/or pictures, which have been reproduced in black and white.

- This document is paginated as submitted by the original source.

- Portions of this document are not fully legible due to the historical nature of some of the material. However, it is the best reproduction available from the original submission.

X-660-77-203
PREPRINT

TMX 71380

ADIABATIC HEATING IN IMPULSIVE SOLAR FLARES

CHRISTIAN MÄTZLER
TAEIL BAI
CAROL JO CRANNELL
KENNETH J. FROST

AUGUST 1977

GSFC — GODDARD SPACE FLIGHT CENTER —
GREENBELT, MARYLAND

X-660-77-203
Preprint

ADIABATIC HEATING IN IMPULSIVE SOLAR FLARES

Christian Mätzler*
Taeil Bai**
Carol Jo Crannell
Kenneth J. Frost

August 1977

*Swiss National Science Foundation Fellow.
**Research supported by NASA Grant 21-002-316 at the University of Maryland, College Park.

GODDARD SPACE FLIGHT CENTER
Greenbelt, Maryland

ADIABATIC HEATING IN IMPULSIVE SOLAR FLARES

Christian Mätzler*
Taeil Bai**
Carol Jo Crannell
Kenneth J. Frost

ABSTRACT

The dynamic X-ray spectra from 28 to 254 keV of two simple, impulsive solar flares are examined together with Hα, microwave and meter wave radio observations. When the effects of the photospheric albedo are taken into account, the X-ray spectra of both events are characteristic of thermal bremsstrahlung from single-temperature plasmas with $10\,\mathrm{keV} \leqslant T \leqslant 60\,\mathrm{keV}$. The symmetry between rise and fall, reported by Crannell et al. (1977), is found to hold not only for the intensity but also for the temperature and emission measure. The relationship between temperature and emission measure is that of an adiabatic compression followed by adiabatic expansion; the adiabatic index of 5/3 indicates that the electron distribution remains isotropic. Observations in Hα provide further evidence for compressive energy transfer, in that both flares show explosive expansion after the end of the intense X-ray spikes. Under the assumption that the X-ray and microwave emissions are produced in the same thermal plasma, the projected areas of the two flares are determined, and the volumes are estimated. Emission measure and electron densities for these events are found to be $n_e^2 V \approx 10^{45}\,\mathrm{cm}^{-3}$ and $n_e \approx 10^9\,\mathrm{cm}^{-3}$, respectively. The strong self-absorption of gyrosynchrotron radiation in a hot plasma is indicative of relatively low magnetic field strengths, $B \approx 100\,\mathrm{G}$. The resulting high beta plasmas inside the source regions are shown to be consistent with the single temperature hypothesis. The nonthermal end phase observed in one event can be explained by the ejection of hot flare plasma or by a second stage acceleration process.

*Swiss National Science Foundation Fellow.

**Research supported by NASA Grant 21-002-316 at the University of Maryland, College Park.

CONTENTS

ILLUSTRATIONS

TABLES

ADIABATIC HEATING IN IMPULSIVE SOLAR FLARES

1. INTRODUCTION

The first rapid increase in the intensity of solar flare radiation lasts typically between 5 and 100 s. This short duration of the impulsive phase has been the main argument for a nonthermal acceleration process (Bowen et al., 1964; Kane and Anderson, 1970; Kahler, 1975). The arguments against a thermal interpretation of the impulsive flare phase have been related to the duration because the heating processes have been assumed to be due to the dissipation of macroscopic energy. The subsequent state of thermalization would be reached only after an appropriate relaxation time, for example the classical self-collision time for electrons in a plasma (Spitzer, 1962). Since in many situations this time is longer than the duration of the observed burst, the electron distribution would not be thermally relaxed.

Apart from microscopic plasma turbulence which can lead to much faster relaxation to a quasi-thermal state (e.g. Spicer, 1976), there is one and only one heating process which is not due to dissipation and therefore does not require subsequent relaxation: *adiabatic compression*. This reversible process does not change a Maxwellian distribution function, but only affects the temperature and density, which are related by the adiabatic equation. A process is adiabatic if the rate of heat loss is negligible compared with the rate of compressive energy transfer. Rapid phenomena, such as the impulsive phase of solar flares, are likely to satisfy this criterion and may therefore be adiabatic.

Chubb (1970) also mentioned adiabatic compression as a heating process which does not produce any nonthermal component in the electron spectrum. This was however ignored by Kahler (1971), who argued against a thermal mechanism being responsible for impulsive solar flares. The only explicit approach to an adiabatic, albeit nonthermal, flare interpretation was made by Brown and Hoyng (1975) by applying the betatron acceleration process to the interpretation of the complex time profile of the great flare of 1972 August 4. Their assumption of a nonthermal electron distribution led to the result that a large fraction of the electrons must populate the power law distribution function above 25 keV. Such a plasma does not deviate strongly from a thermal state at a temperature above 20 keV, because the mean electron energy is close to the mean energy of the high energy component.

The tendency for short duration processes to be purely adiabatic makes it attractive to investigate flare phases of short duration. This idea is supported by Chubb (1970) who found the spectrum of the impulsive X-ray phase of a disruptive prominence consistent with the bremsstrahlung spectrum of a plasma at a single

temperature. The same result was found for the majority of 22 impulsive X-ray flares by Crannell et al. (1977), hereinafter referred to as Paper 1.

Strong support for an adiabatic heating and cooling process comes from the symmetry between rise and fall times of the impulsive X-ray bursts analyzed in Paper 1. The symmetry implies that the process responsible for the decay must be the same as the process which determines the rise. Although this does not exclude dissipative processes over time scales much longer or much shorter than the rise and fall times, irreversible processes are unlikely to be responsible for the observed time structure of these events. Hence a reversible process must determine the dynamics of impulsive X-ray bursts. The only heating process which is both thermal and reversible is adiabatic compression.

The occurrence of adiabatic processes can be tested by direct observation of the compression and expansion and by comparison of the changes observed simultaneously in temperature and volume. Since the observed temperatures of impulsive X-ray flares are in the range 10 to 100 keV, the observable radiation from the electron-proton plasma is collisional and magneto-bremsstrahlung, the latter also being called gyrosynchrotron radiation. The optimum frequencies for observing both kinds of radiation are in the hard X-ray and microwave ranges. These observations are restricted mainly to the spatially integrated radiation of the whole flare region. Because the adiabatic equation of a single temperature plasma can be written in terms of temperature and spatially integrated emission measure, tests can be made from observations without spatial resolution. If they exist at all, single temperature situations are most likely to be present in simple flares. The impulsive flares of Paper 1 are favorable, because they show only single spikes; however, only the two largest events have sufficiently high photon rates to test the single temperature hypothesis and to allow a determination of the dynamic spectra. These two flares are discussed in Sections 3 and 4. The results are consistent with an adiabatic flare source whose properties are discussed in Section 5. In Section 2 an accurate approximation to the hard X-ray spectrum of a thermal source in the solar atmosphere is developed.

2. DERIVATION OF X-RAY FLARE PARAMETERS

According to Tucker (1975), the differential X-ray flux of a thermal electron-proton plasma, emitting optically thin free-free radiation, is related to the temperature, T, and the emission measure, $EM \doteq n_e^2 V$, where n_e is the electron density and V the volume of the source. At a distance of $150 \cdot 10^6$ km from the source the differential X-ray flux $I_s(E, T)$ in units of photons $cm^{-2}\ s^{-1}\ keV^{-1}$ is given by

$$I_s(E, T) = 1.07 \cdot 10^{-42} \frac{EM}{E\, T^{1/2}}\, g_{ff}(E, T) \exp(-E/T) \qquad (1)$$

where the photon energy, E, and T are in keV, EM in cm^{-3}, and the Gaunt factor, $g_{ff}(E, T)$, is a dimensionless correction factor.

Because we are interested in the exact relationship between EM and T as a function of time, it is important to calculate them as accurately as possible, noting the difficulty that an overestimate of one quantity results in the underestimate of the other. Such an effect distorts any correlation between the two parameters. We have, therefore, improved upon the parameter-estimation technique presented in Paper 1 by taking into account the relativistic Gaunt factor and the backscattering of photons from the photosphere. The effect of the finite energy resolution of the detector has been taken into account for the steep spectra as shown in Section 4. The Gaunt factor and the photospheric albedo are discussed in the following subsections.

2.1. The Gaunt Factor

We have derived Gaunt factors for free-free emission from an optically thin, thermal proton-electron plasma using the relativistic Maxwell distribution and the bremsstrahlung cross section formula given by Koch and Motz (1959, Equation 3BN). The results for a range of temperatures and photon energies are shown in Table 1, together with an empirical fit for the Gaunt factor $g_{ff}(E, T)$, which is given by

$$g_{ff}(E, T) \approx 0.90 \left(\frac{T}{E}\right)^{\alpha}, \qquad (2)$$

where

$$\alpha = 0.37 \left(\frac{30\ \text{keV}}{T}\right)^{0.15}$$

Table 1

Gaunt Factors $g_{ff}(E, T)$, Compared With the Approximation of Equation (2)

$E_{(keV)}$	T = 15 keV		T = 30 keV		T = 50 keV	
	Exact	Eq. (2)	Exact	Eq. (2)	Exact	Eq. (2)
10	1.037	1.063	1.316	1.35	1.557	1.562
15	0.893	0.900	1.150	1.163	1.381	1.360
20	0.799	0.800	1.039	1.046	1.260	1.232
30	0.679	0.677	0.896	0.900	1.100	1.072
50	0.548	0.549	0.736	0.745	0.917	0.900
70	0.474	0.478	0.645	0.658	0.811	0.802
100	0.406	0.413	0.558	0.576	0.713	0.710
150	0.343	0.350	0.481	0.496	0.620	0.618
200	0.307	0.311	0.438	0.446	0.569	0.560
300	0.273	0.263	0.397	0.384	0.523	0.487

2.2. Backscattering From the Photosphere

The photospheric albedo due to Compton scattering of photons from a primary X-ray source has been shown to be important, mainly at photon energies near 30 keV (Tomblin, 1972; Santangelo, Horstman and Horstman-Moretti, 1973; Langer and Petrosian, 1977; Bai and Ramaty, 1977). Because this energy is the lowest X-ray energy of data used here, the effect of the backscattering is a steepening of the source spectrum. The coefficient describing the intensity of the reflected photons depends on the spectrum of the primary photon source, on the energy of the reflected photons and on the angle θ between the direction of observation and the normal to the photosphere at the position of the flare.

For thermal spectra with temperatures between 20 keV and 100 keV Bai and Ramaty (1977, Figure 1) give a reflection coefficient $\bar{R}(E, T)$ averaged over all

directions θ. The curves are well represented by the following functional form for $\bar{R}(E, T)$:

$$\bar{R}(E, T) = \begin{cases} \left[0.21 + 0.31\left(\frac{T}{30\,keV}\right)^{0.4}\right] \cdot \ell n\left(0.5 + \frac{E}{14.3\,keV}\right), & 10\,keV < E < 32\,keV\,; \\ \max\left\{0.0,\ 0.31\left(\frac{T}{30\,keV}\right)^{0.4} - 0.34\,\ell n\left(\frac{E}{60\,keV}\right)\right\}, & E > 32\,keV\,. \end{cases} \tag{3}$$

$\bar{R}(E, T)$ increases with increasing temperature and has a maximum at an energy E of 32 keV. To find the reflection coefficient $R(\theta, E, T)$ for a certain flare position it is assumed that

$$R(\theta, E, T) = C(\theta) \cdot \bar{R}(E, T) \tag{4}$$

This simplification is a good approximation when we use the empirical function $C(\theta)$ shown in Figure 1 as a function of $\sin\theta$. Although for large values of θ this approximation is not so good, the error in the total flux due to this approximation is negligible, because $R(\theta \approx \pi/2, E, T)$ is small. Note that $\bar{R}(E, T)$ can, in principal, be larger than unity, although the mean value over all energies is less than unity. The total differential X-ray flux is given by

$$I(\theta, E, T) = (1 + R(\theta, E, T)) \cdot I_s(E, T) \tag{5}$$

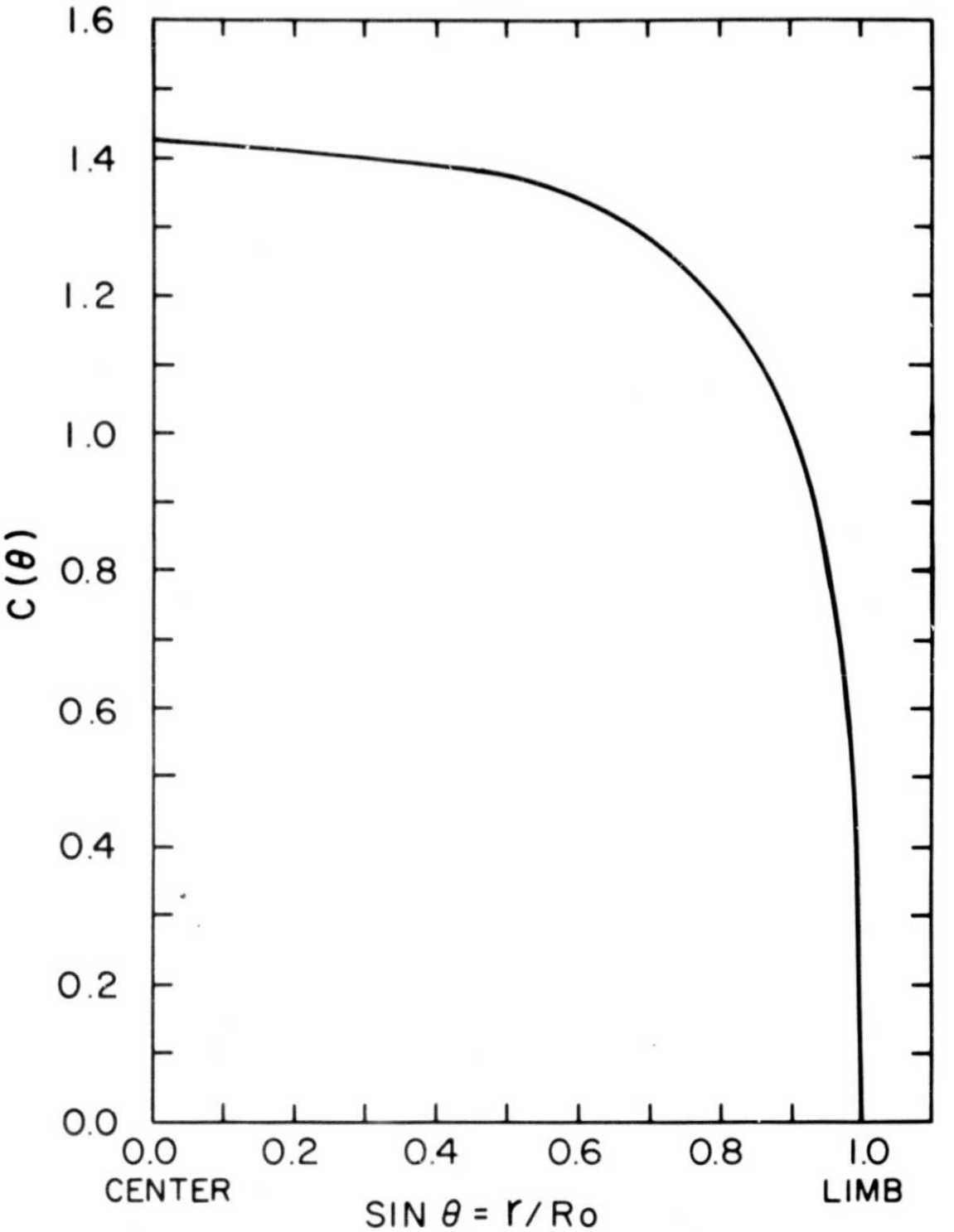

Figure 1. The function $C(\theta)$, describing the influence of the flare position on the albedo. R_0 is the radius of the sun and r is the distance of the flare source from the center of the solar disk.

3. THE FLARE OF 1970 MARCH 1

3.1. General Description

Of the spike bursts presented in Paper 1, the flare with the largest emission in Hα, in microwaves, and in X rays is the flare of 1970 March 1. This event is discussed here.

The Hα flare starts at about 1126 UT in the brightest region of McMath Plage 10595, in the western solar hemisphere. The flare structure is a system of loops in a nearly circular area with a diameter of 50,000 km. After 1128 UT the flash phase brightening is followed by an explosive phase reaching a maximum of importance 2B two minutes later. In Figure 2 the flare is shown in Hα at the beginning of the explosive phase and at maximum, as observed at the Zurich Observatory. A gradual increase of both hard X-ray and microwave emission (Figures 3 and 4) starts shortly after 1126 UT together with a series of type U radio bursts at frequencies between 180 and 400 MHz. The U-burst association is typical for those X-ray events in Paper 1 with correlated meter wave emission. It is reasonable to assume that the X-ray flare source is a plasma strongly confined by magnetic fields because U-burst exciters are generally believed to be electron beams traveling through closed coronal loops. Only during the intense X-ray maximum phase at 1127:45 UT are large coronal heights involved in the flare disturbance; this is shown by the broadband emission in the radio spectrogram of Figure 3, in which the radiation extends to wavelengths of at least up to 10 m.

As shown in Figure 4, the 10.5 GHz microwave and the relative X-ray fluxes of 28 to 82 keV photons agree very well in their time profiles. The only deviation in Figure 4 takes place after 1128 when a microwave post-burst increase starts to dominate; at the same time the hard X-ray spectrum begins to deviate from that of a single temperature plasma, as is shown in Section 3.2.

The explosive expansion of the Hα flare region at the end of the impulsive burst is connected with a strong shock resulting in type II burst radiation as shown in Figure 3. That this phase is not correlated with an effective second stage acceleration is inferred from the lack of enhanced hard X-ray emission.

Although the flare position is favorable for direct particle observations, no particle event is reported. This implies that the energetic particles are trapped in the closed magnetic fields of the active region, a situation which favors particle acceleration by a compressive disturbance.

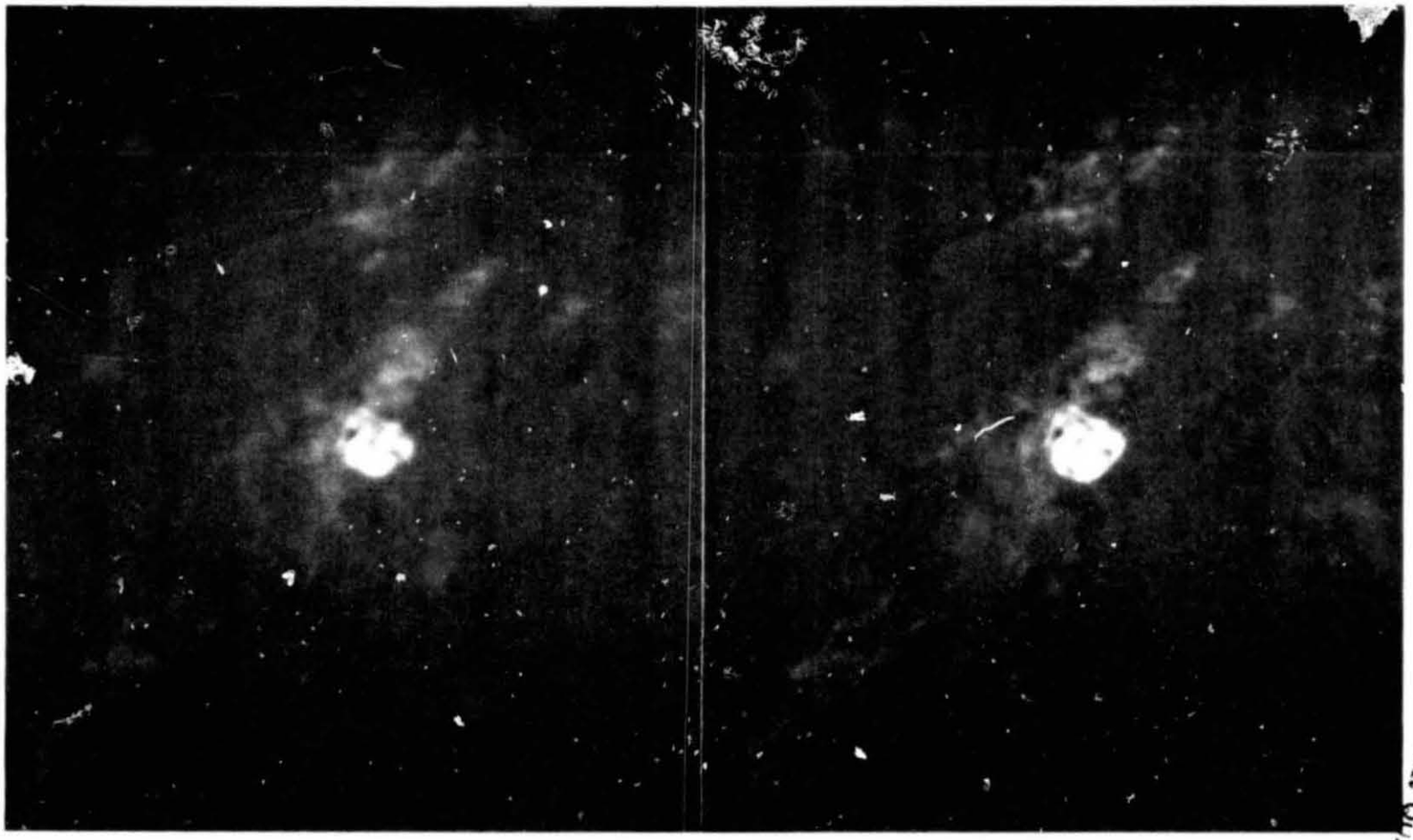

Figure 2. Flare in Hα on 1970 March 1 at the position N13, W31 (Solar Geophysical Data). West is on the top, north at the left of the photographs. (Courtesy of M. Waldmeier, Zürich).

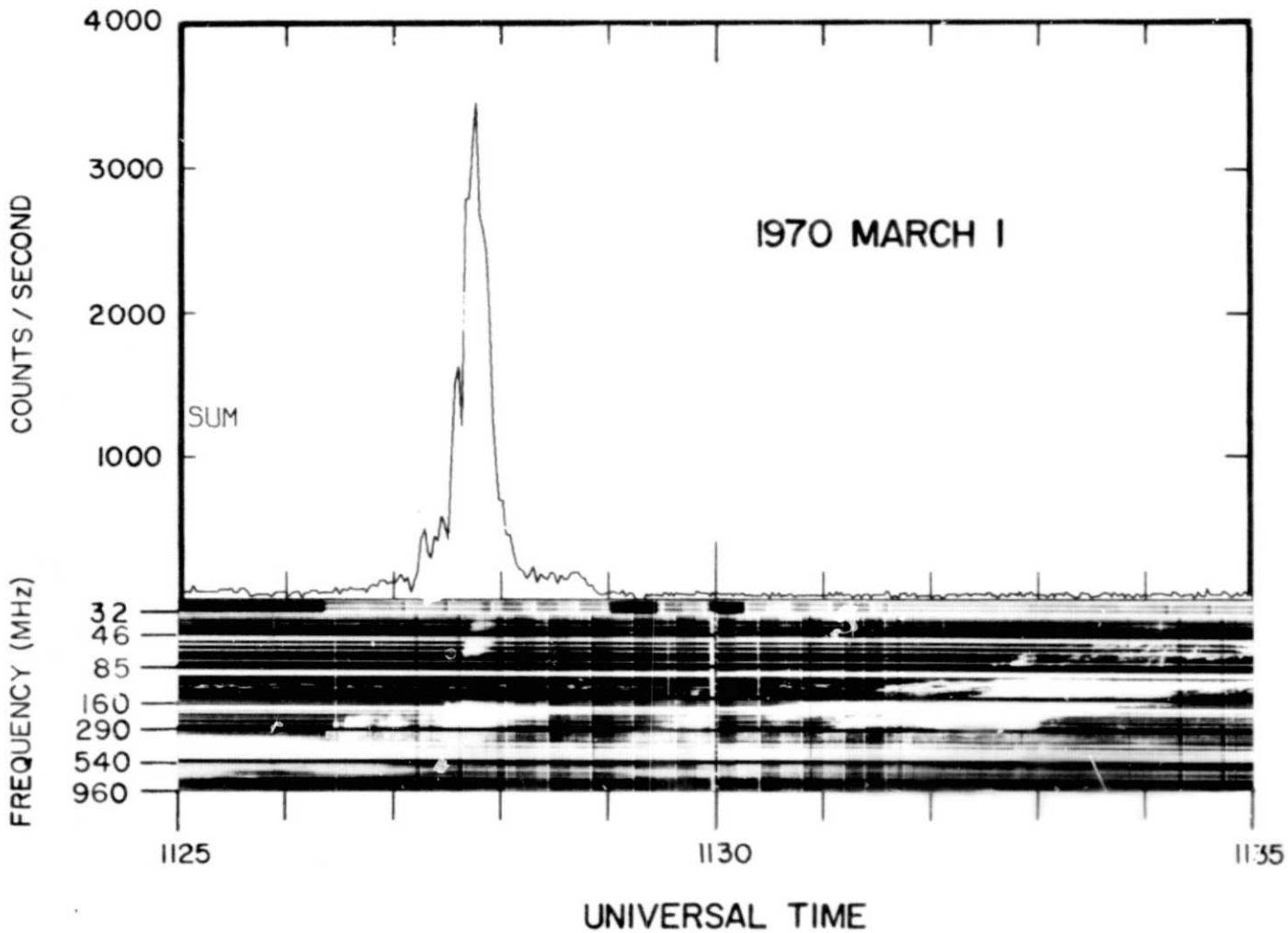

Figure 3. Radiospectrogram (Courtesy of H. Urbarz, Weissenau) and total count rate of the OSO-5 X-ray spectrometer. The reduced brightness in the range 85 to 160 MHz is due to a lower sensitivity of the radio spectrometer.

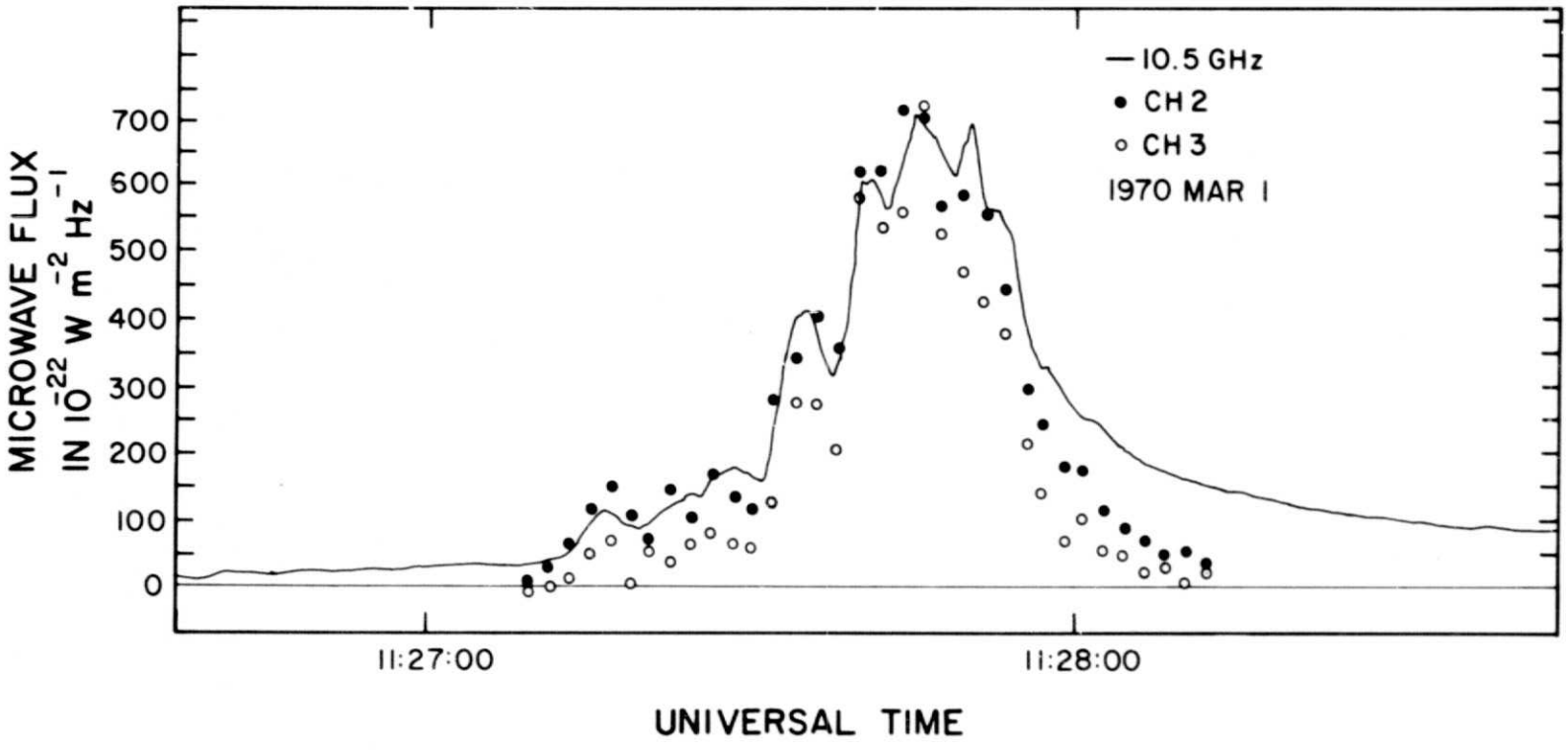

Figure 4. Microwave time profile at 10.5 GHz with a time constant of 0.2 s (Courtesy of A. Magun, Bern) compared with the X-ray fluxes of Channel 2 (28-55 keV) and Channel 3 (55-82 keV), normalized to the maximum of the microwave flux.

3.2. The Adiabatic X-ray Phase

In Figure 5 the hard X-ray spectrum for the 2 s interval at time of maximum is shown. Crosses represent the total observed flux, including the source plus albedo observed in Channels 2 to 8 of the OSO 5 spectrometer; circles with statistical uncertainties show the deduced source spectrum. It is compared with a best-fit bremsstrahlung spectrum of a plasma at the temperature T = 57 keV. The lowest channel (14-28 keV) is not included, because its calibration is uncertain and strongly dependent on the actual low energy spectrum. Channel 9 (225-254 keV) also has been excluded, because the statistical uncertainty is too large. The data of the remaining channels are plotted at their effective mean photon energies. The goodness of the thermal fit shown in Figure 5 is typical for the time between 1127:30 and 1128:00 UT, during which the intensity in Channel 2 is above 1/4 of maximum. The χ^2-tests of all fits together give a total value $\chi^2 = 40$ with the total degree of freedom $N_f = 52$; the probability that the deviations of the data from thermal spectra are by chance is about 80%. Attempted fits to power law spectra for the same data have a total $\chi^2 = 107$; the probability that the data deviate from power law spectra only by chance is less than 10^{-3}. The parameter fits were made as a function of time from a running mean over pairs of data samples. The temperatures, T_{2j}, were calculated from the ratios of the fluxes in Channel 2 and Channel j; $j = 3, j_{max}$. The uncertainties, ΔT_{2j}, were determined from the statistical uncertainties in the fluxes of Channels j. The small uncertainty in Channel 2 and systematic errors due to the calibration of energy and efficiency were neglected. In Figure 6 the derived mean temperature and emission measure are plotted together with the high time resolution record of the 10.5 GHz flux. For times after 1128 the temperature T_{23}, instead of the mean, T, is plotted, and the average value of T_{25} of the whole end phase is shown for comparison. The clear enhancement of T_{25} with respect to T_{23} indicates the presence of a multithermal or non-thermal plasma; this phase is discussed in Section 3.4. The time variations of the temperature, the emission measure and the microwave flux are similar; even the microwave fine structure is reflected in the temperature fluctuations.

In Figure 7 the correlation diagram between EM and T is shown; the arrows indicate the direction of increasing time. The data points follow almost the same line during rise and fall. This behavior supports the hypothesis of a reversible flare process during the impulsive phase as found in Paper 1 from the symmetry between rise and fall times. The dashed line in Figure 7 is the predicted relation between EM and T for an adiabatic heating and cooling process with an adiabatic index 5/3, corresponding to a plasma with an isotropic electron distribution (see Section 5.3.). The good agreement of the data with this line shows that adiabatic energy transfer is consistent with the dynamic X-ray spectrum. The apparent isotropy of the electrons in the compressed and expanded plasma region does not exclude the presence of anisotropic electron beams which have escaped

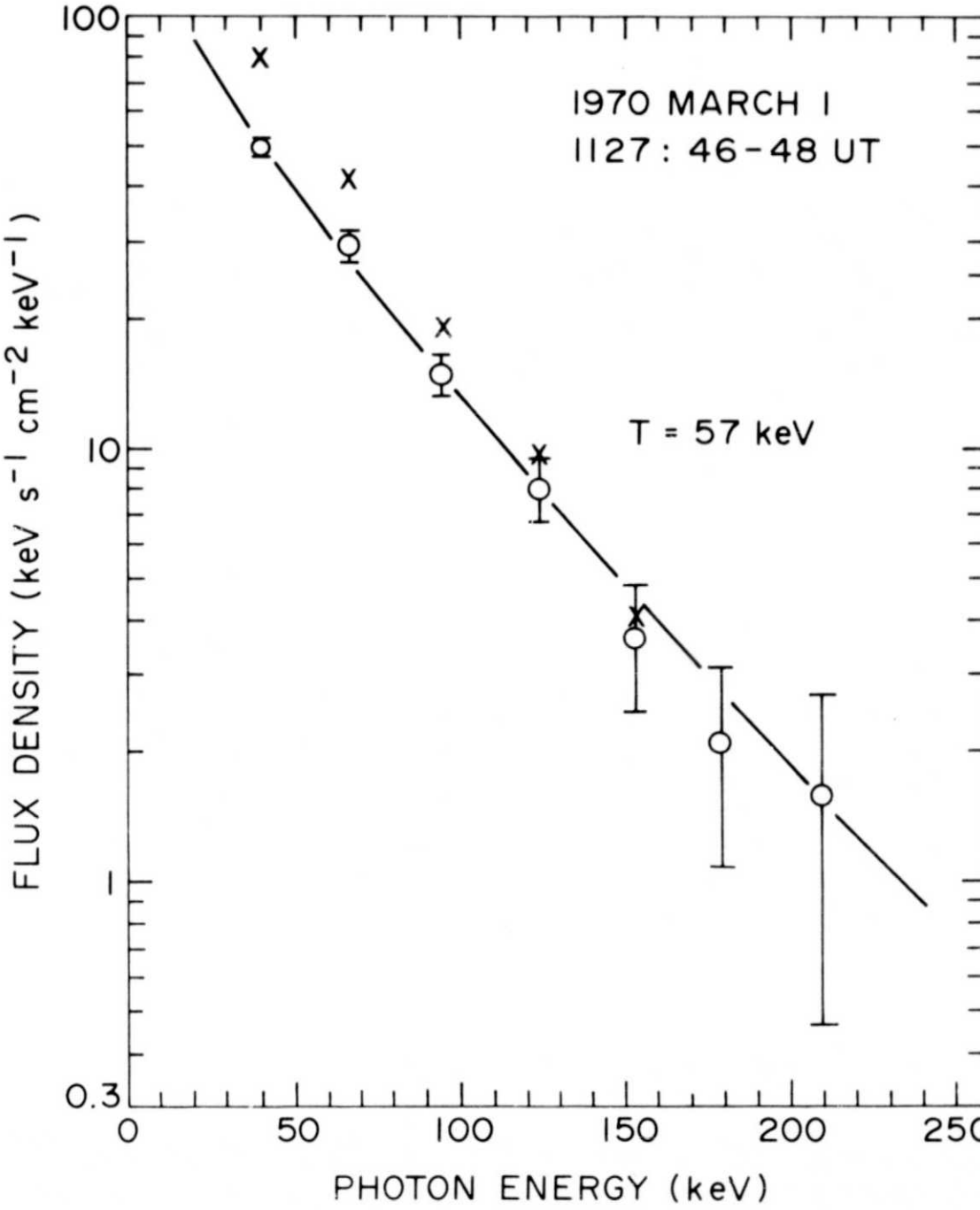

Figure 5. Hard X-ray photon energy spectrum at time of maximum intensity. Crosses represent the total flux. The direct flux from the source (circles with uncertainties) is calculated by subtracting the albedo. The resulting spectrum is fitted to optically thin free-free emission of a single temperature plasma with T = 57 keV and EM = $0.8 \cdot 10^{45}$ cm^{-3} (solid line).

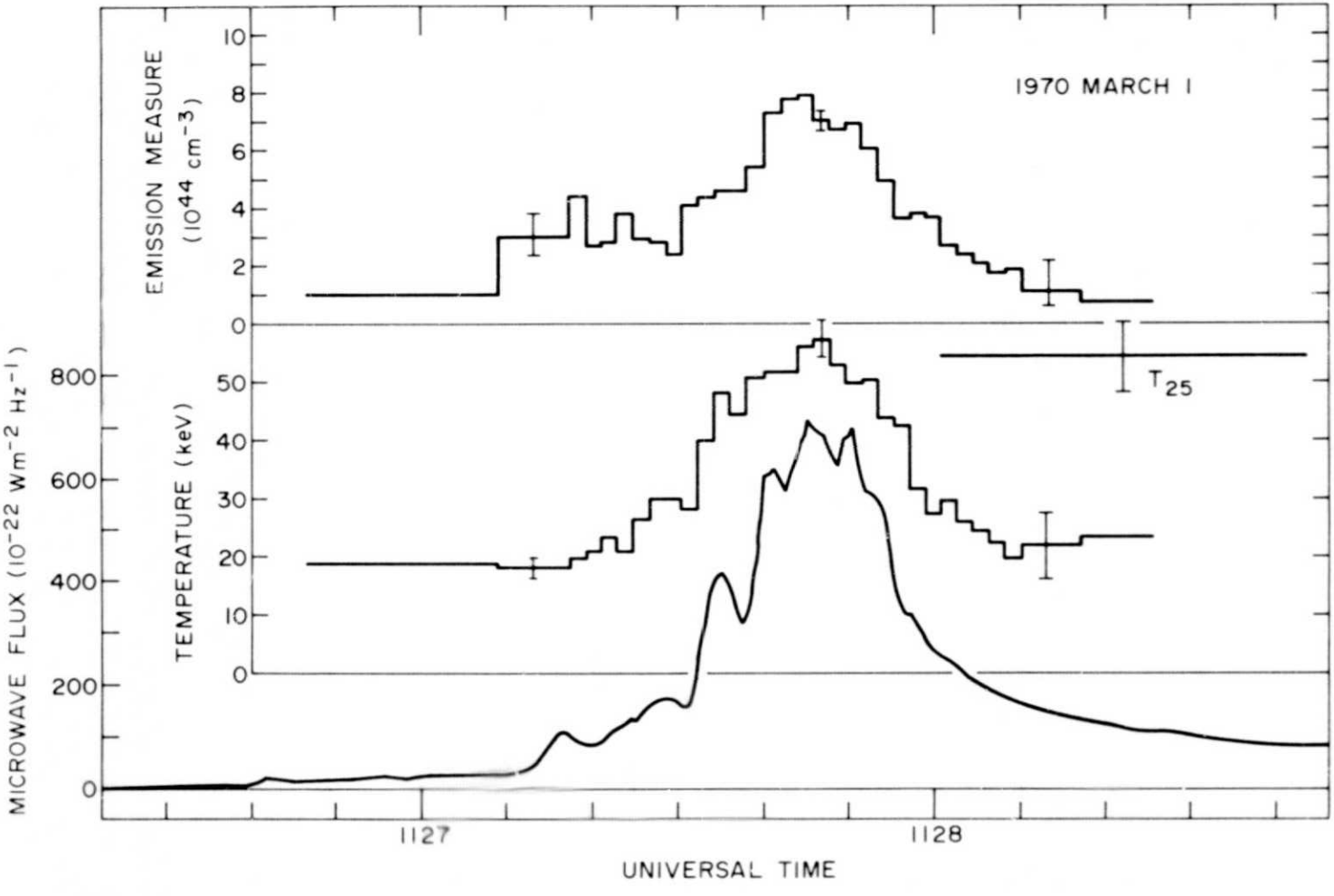

Figure 6. Time profiles of the emission measure EM and temperature T, as derived from the X-ray spectrum, and compared with the 10.5 GHz flux. During the nonthermal end phase, after 1128 UT, the temperature of the flare source is approximated by T_{23}, and T_{25} represents the average value of the temperature derived from Channels 2 and 5 (28–55 keV and 111–141 keV).

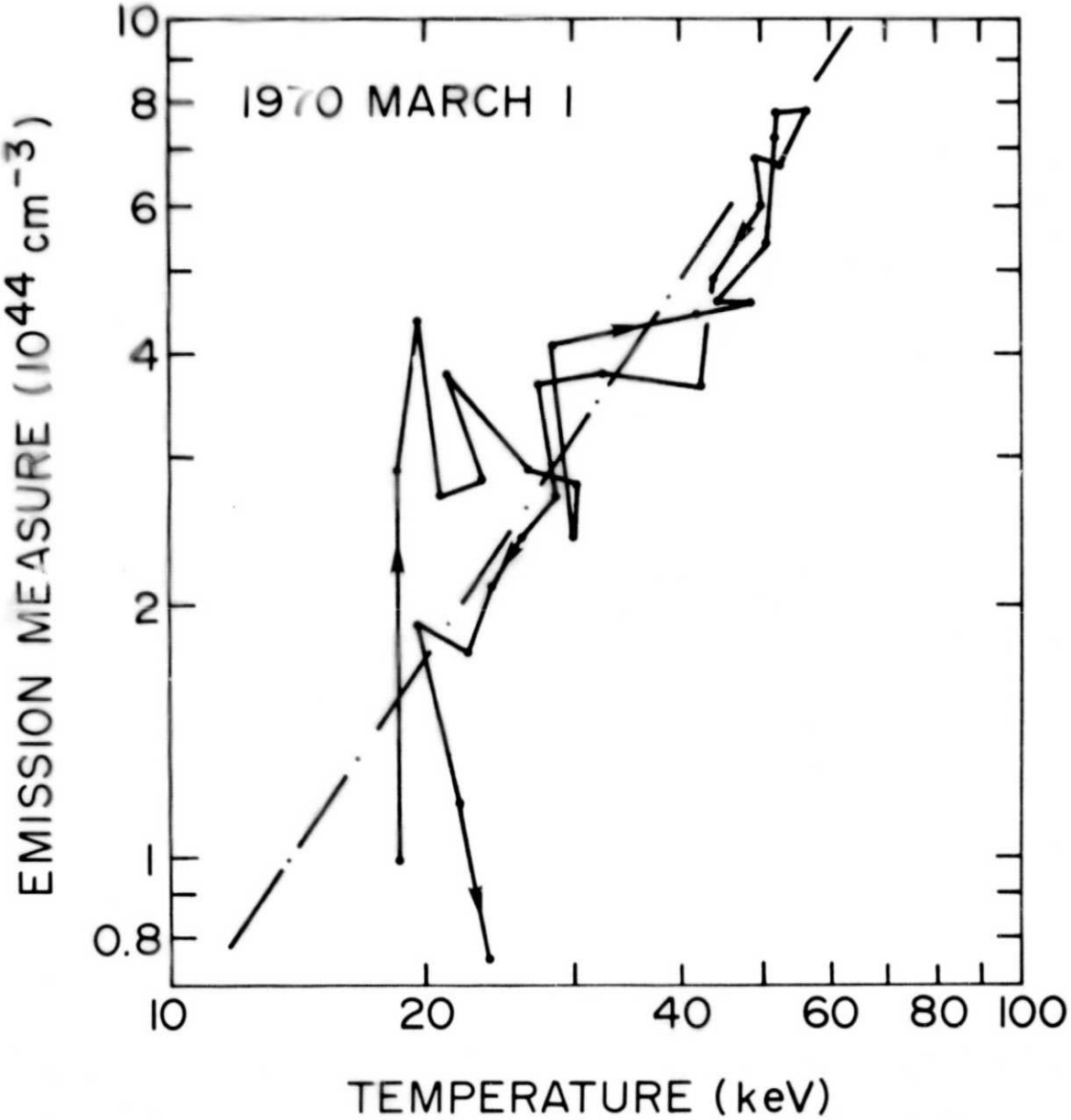

Figure 7. Correlation diagram between EM and T. The dashed-dotted line represents the relationship for an adiabatic process with adiabatic index $\kappa = 5/3$.

from that region. Such beams could account for the observed low frequency radio emission, as well as for some of the X-ray photons as a result of injection into a thin or thick target. In the case of the flare under consideration the number of escaping electrons must be so small that the adiabatic and reversible character of the maximum phase is conserved.

3.3. The Microwave Spectrum and Flare Parameters

The excellent agreement of the X-ray and microwave time profiles implies that both kinds of radiation are emitted from the same region with volume V and projected area A. Because in an isotropic compression V varies proportional to $A^{3/2}$ and given the adiabatic equation, $T\,V^{2/3}$ = constant, A T does not vary with time. Furthermore, because the low-frequency black-body intensity is proportional to $A\,T\,f^2$ we arrive at the interesting conclusion that an observer looking at a frequency, f, at an optically thick source undergoing an isotropic, adiabatic change does not see a change in intensity. An interesting by-product of this analysis is that the low frequency, optically thick, part of the microwave spectrum may be useful for studying secondary phenomena, such as time-dependent occultation of the background radiation and optically thin radiation from outer regions. At higher frequencies the strongly temperature dependent emissivity of gyrosynchrotron radiation dominates the flux variation, similar to the effect of temperature variation on the free-free emissivity in the hard X-ray range. A detailed calculation of microwave spectra, based on the work of Ramaty (1969), is in preparation by one of the authors (C. M.).

The microwave spectrum of the flare under consideration is not well known; the records from Sagamore Hill Observatory are heavily distorted by interference due to the sun rise, and records from other observatories have an insufficient time resolution for a dynamic study with the exception of the 10.5 GHz data from Bern, which are shown in Figures 4 and 6.

At the time of maximum intensity the spectrum is consistent with an f^2-law near 3 GHz, has a maximum between 5 and 9 GHz, and decays from $700 \cdot 10^{-22}$ W m^{-2} Hz^{-1} at 10.5 GHz to $400 \cdot 10^{-22}$ W m^{-2} Hz^{-1} at 19 GHz. From the mean value of the reported fluxes, $S(3\,\mathrm{GHz}) = 400 \cdot 10^{-22}$ W m^{-2} Hz^{-1}, and the previously derived temperature T = 57 keV, we find with Formula (9) of Paper 1 that

$$A = 5 \cdot 10^{18}\ \mathrm{cm}^2 .$$

This projected area is 1/4 of the measured Hα flare area during the flash phase. Both areas are the largest observed and derived areas of all the impulsive flares of Paper 1.

The time variation of the microwave area cannot be determined, but there is a clear indication that the variation of the microwave flux is slower at lower frequencies; in particular below 3 GHz the flux changes more slowly than the temperature shown in Figure 6. If the source is optically thick at these frequencies, it is smaller at burst maximum than at other times.

Assuming that the volume $V = KA^{3/2}$, where K is a constant of order unity in an isotropic geometry, we find for the maximum phase $V = 10^{28}\,K\,cm^3$; and with the emission measure $EM = 8 \cdot 10^{44}\,cm^{-3}$ the electron density is found to be $n_e = 3 \cdot 10^8/K^{1/2}\,cm^{-3}$. The total number of electrons is $N_e = 3 \cdot 10^{36}\,K^{1/2}$; assuming equipartition of energy between ions and electrons the total thermal energy is $U = 8 \cdot 10^{29}\,K^{1/2}$ erg. For K = 1 the density is small, but it must be kept in mind that we assumed the very simplified model of a homogeneous source with an isotropic geometry. If the source is a sheet perpendicular to the line of sight, K is very small, equal to the ratio of sheet thickness to sheet diameter.

The microwave spectrum can also be used to determine the magnetic field strength in the flare source. The high plasma temperature keeps the microwave source optically thick up to high harmonics of the gyrofrequency. For such high temperature plasmas (T = 50 keV) of solar flare dimensions, the peak frequency is approximately 30 times the electron gyrofrequency (Drummond and Rosenbluth, 1963). The peak frequency of ~7 GHz implies, therefore, that the characteristic magnetic field of the emission region, B, is approximately 80 G. The magnetic energy $B^2/8\pi = 260\,erg/cm^3$ is only three times the kinetic energy density, U/V, for K = 1. Since K is of order unity or less we find a situation of a high beta plasma, that is a plasma with approximate equipartition between kinetic and magnetic energies. This explains the irregular fluctuations of the microwave signal due to the high level of magnetohydrodynamic turbulence and may be a clue to the instability leading to adiabatic compression.

3.4. The Nonthermal End Phase

During the end phase of the X-ray burst, after 1128 UT, the derived temperatures increase with increasing photon energy, and in the power-law fit the absolute values of the derived spectral indices decrease with increasing energy. In Figures 6 and 7 the lowest temperature T_{23} has been used to describe the adiabatic expansion during the end phase. The temperature T_{23} may be most closely related to a physical temperature in the flare source because the hardening at higher energies is thought to be due to a superimposed high energy tail of electrons. These may be produced during or after the impulsive phase, or they may be a residual energetic component of electrons which are not subject to the adiabatic deceleration.

The first explanation is supported by a possible second stage acceleration by the expanding shock. The existence of this shock is manifested by the type II burst shown in Figure 3 and by the explosive phase of the Hα flare. However, the post-impulsive enhancement in hard X-rays is very small compared with other flares (e.g. Frost, 1969).

Therefore the second explanation also will be considered: a natural deviation from a purely adiabatic behavior can occur in a flare source in which a few electrons are allowed to escape into an extended halo. In fact the nonthermal meter-wave burst during the impulsive phase shows that electrons escape into high coronal regions. During the end phase shown in Figure 6 the mean flux of photons with energy larger than 100 keV is 5% of the flux during flare maximum. Therefore 5% of electrons with energies larger than 100 keV must escape if the density is the same in both source and halo. The number of escaping electrons is so small that the main process still appears to be adiabatic, and the electron distribution in the source remains close to Maxwellian. The life time of the escaping electrons is determined by non-adiabatic energy losses and may well correspond to the observed duration of the end phase, because the collisional energy loss time of 100 keV electrons in a plasma with density $n = 10^9/cm^3$ is about 100 s (Benz and Gold, 1971). The same electrons can also account for the microwave post burst phase if the flare source at burst maximum contains regions with high optical depth at 10.5 GHz. Then the microwave post burst is optically thin gyrosynchrotron radiation in the halo. Hoyng (1975) came to the same conclusion from the analysis of a flare on 1972 May 18.

The conclusion common to both explanations for the hard post burst X-ray spectrum is that the end phase is a nonthermal product of the purely thermal maximum phase. This is exactly the reverse of the opinion (e.g. Kahler, 1971) that the rapid and intense impulsive phase must be nonthermal, whereas the end phase is thermally relaxed.

4. THE FLARE OF 1969 MARCH 1

4.1. General Description

The data of the second largest flare of the impulsive bursts in Paper 1 also can be used to study the dynamic X-ray spectrum. The coincident Hα flare starts at 2253 UT, slightly south west of the center of the solar disk. The flare reaches the maximum of importance -N only two minutes later, characterized by an explosive phase.

The X-ray spike burst is shown in Figure 8. Rise and fall times, defined as durations between maximum and 1/4 of maximum intensity, are 6.0 and 6.4 s, with uncertainties of ±1 s. The main spike is clearly symmetric, even the small precursor and similar end phase seem to be a pair of the same phenomenon. The microwave burst peaks together with the X-ray spike, and has a very steep spectrum. No radiation is observed below 3.75 GHz (*Solar Geophysical Data* No. 301, Part II, 1969); the peak frequency is probably higher than 9.4 GHz, at which the maximum observed flux is $95 \cdot 10^{-22}$ W m^{-2} Hz^{-1}. The lack of low frequency radiation implies that the flare region is restricted to low coronal heights, probably to the transition region.

4.2. The Adiabatic X-ray Phase

The hard X-ray spectrum of the flare under consideration is very steep. It is even steeper than the directly deduced pulse height spectrum, because the finite energy resolution of the detector broadens the true X-ray spectrum. For the OSO-5 spectrometer this instrumental effect becomes important for plasma temperatures below 20 keV.

Limited information can also be derived from steeper spectra by taking into account the energy resolution function of the detector. Thermal spectra, enhanced by the photospheric albedo, were convolved with the Gaussian detector response and integrated over the widths of the channels. The result of the fit to the observed pulse height spectrum at burst maximum is shown in Figure 9. Within the statistical uncertainties the fit is consistent with a single temperature plasma with T = 22 keV and EM = $1.6 \cdot 10^{45}$ cm^{-3}. The uncertainty in T is less than 2 keV. The remaining data samples have high statistical uncertainties at high energies, restricting the fit to two or three channels. This does not permit a determination of the spectrum, although a single temperature and emission measure can still be derived. The resulting correlation diagram between the two parameters is shown in Figure 10. The good agreement with the dashed line, representing the predicted correlation due to an adiabatic process, shows that the dynamic X-ray spectrum of the main spike is consistent with an adiabatic compression and subsequent expansion.

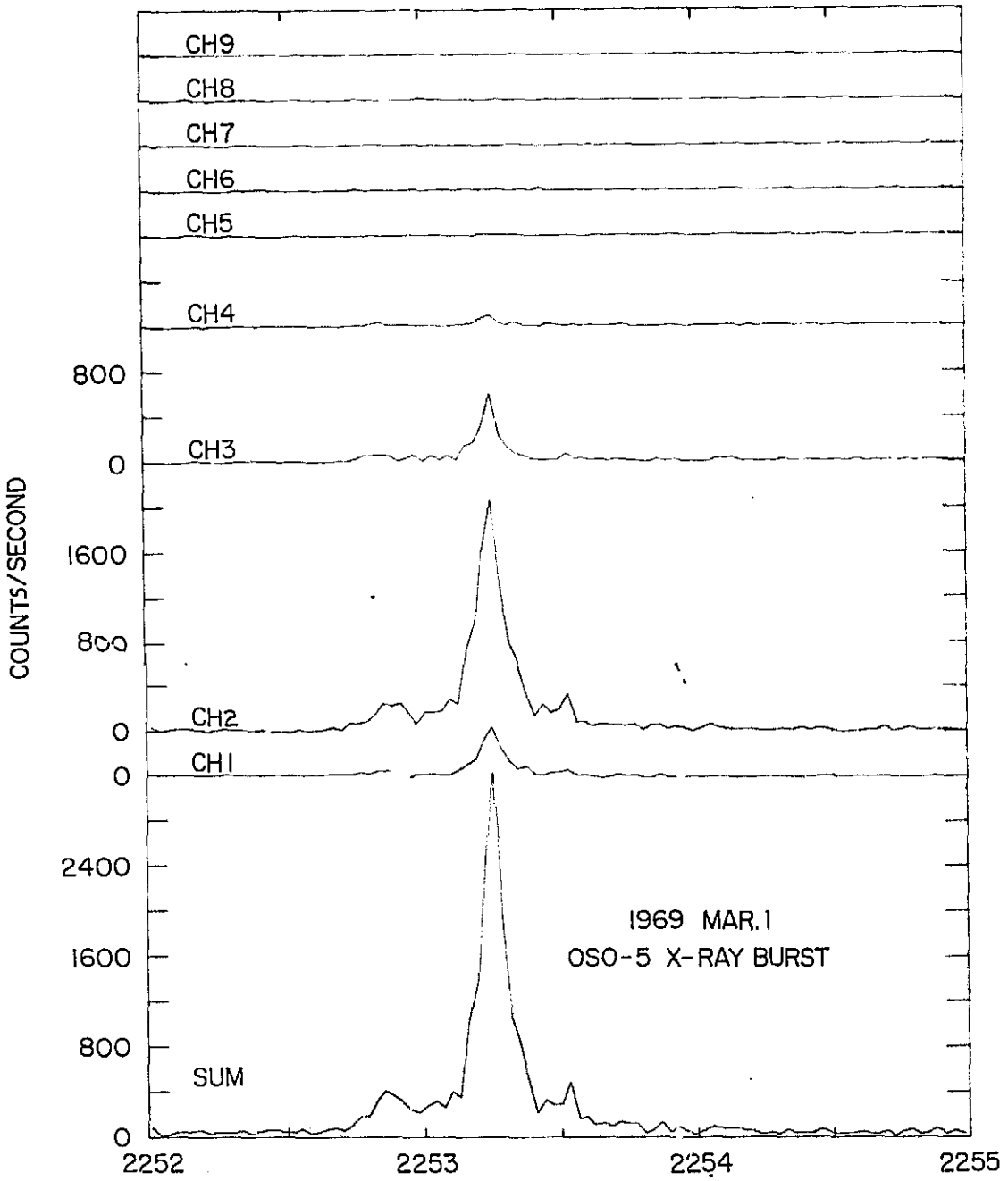

Figure 8. Time history of the X-ray pulse height spectrum during the impulsive flare of 1969 March 1. The 9 channels represent the energy ranges bounded by subsequent pairs of the following values in keV: 14, 28, 55, 82, 111, 141, 168, 200, 225, 254.

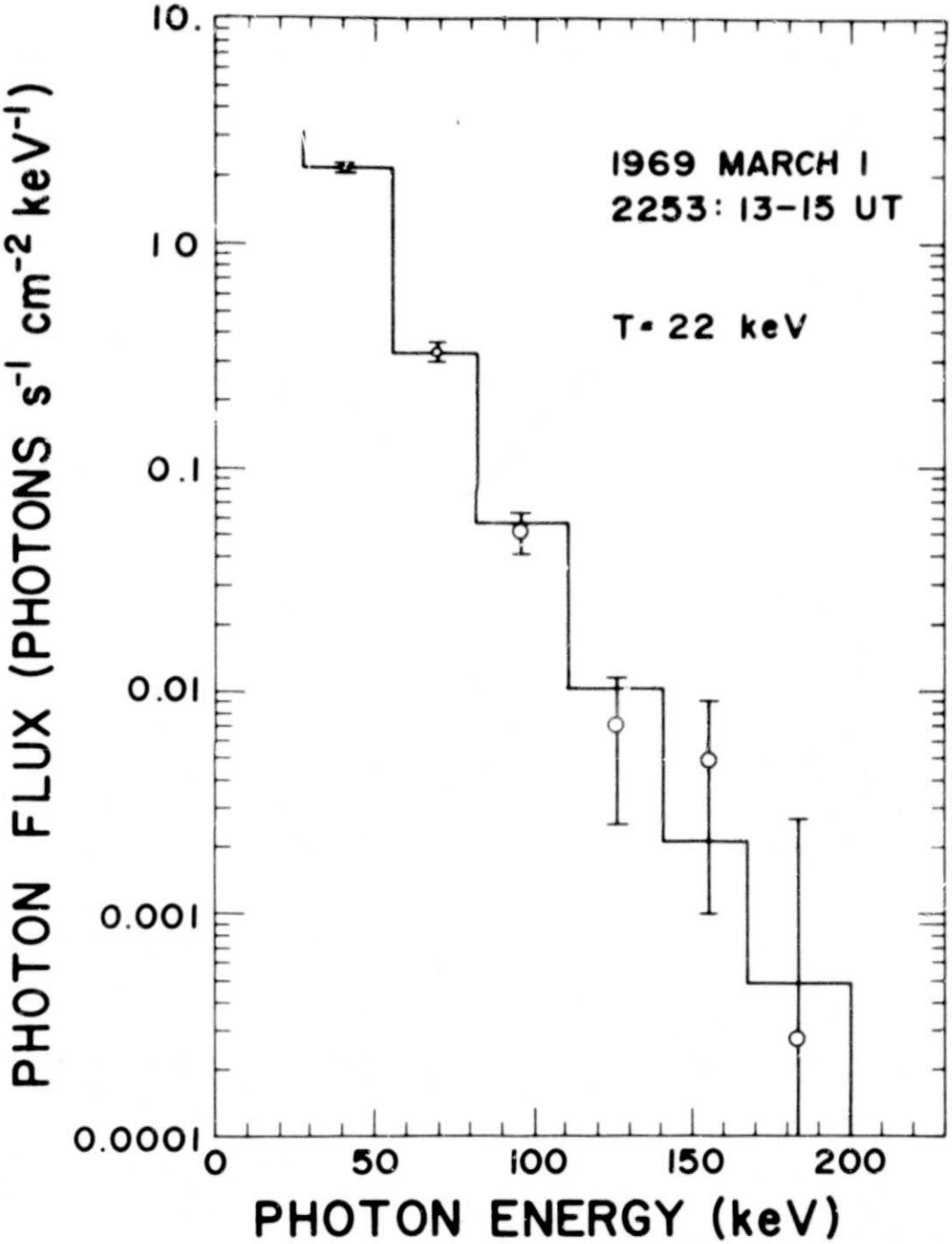

Figure 9. Hard X-ray pulse height spectrum at time of maximum intensity. Circles with uncertainties represent the data. The best fit thermal spectrum ($T = 22\,keV$, $EM = 1.6 \cdot 10^{45}\,cm^{-3}$) including the photospheric albedo, and folded with the detector response, is shown by the solid line.

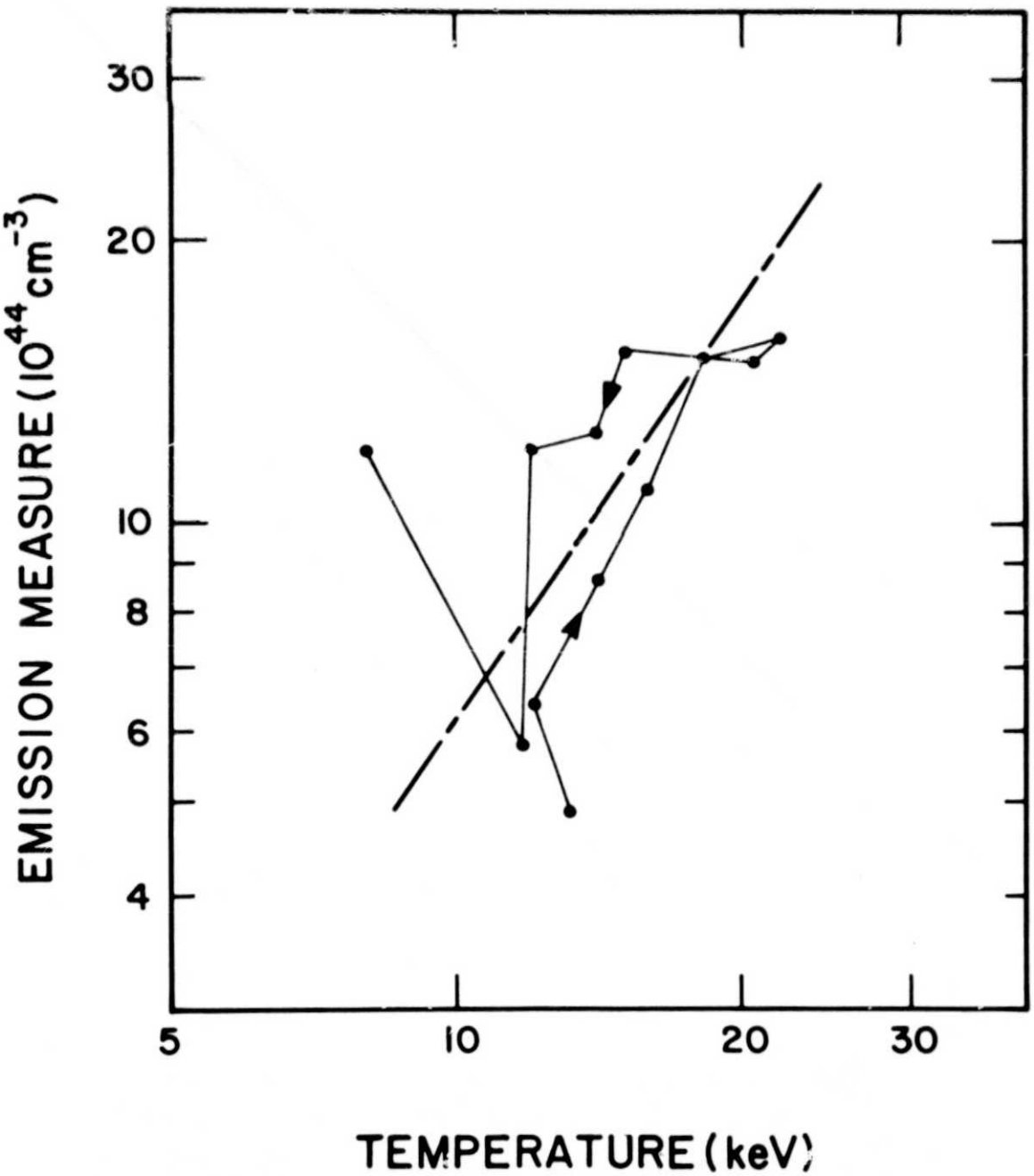

Figure 10. Correlation diagram between EM and T. The dashed-dotted line represents the relation for an adiabatic process with adiabatic index $\kappa = 5/3$.

4.3. Flare Parameters at Time of Maximum and the Relationship to Other Flares

The parameters at the time of maximum can be derived in the same way as in Section 3.3. For a black body of T = 22 keV with a flux of $17 \cdot 10^{-22}$ W m^{-2} Hz^{-1} at f = 3.75 GHz, the area of the source region is $A = 0.34 \cdot 10^{18}$ cm^2. For a geometry factor of K = 1 the volume is $V = 0.2 \cdot 10^{27}$ cm^3, and the electron density is $n_e = 3 \cdot 10^9$ cm^{-3} for the observed emission measure of $EM = 1.6 \cdot 10^{45}$ cm^{-3}. If the ion and the electron temperatures are the same, the total thermal energy of the flare source is $U = 3n_e VkT = 6 \cdot 10^{28}$ erg, and the thermal energy density is 300 erg cm^{-3}. The actual geometry of the source changes the value of the parameters by powers of K, assuming homogeneous sources (see Section 3.3.).

The magnetic field strength in the source region of the flare under consideration must be larger than the field of the flare on 1970 March 1, because the peak frequency is higher. Since the thermal energy density also is higher by a factor of 4, the plasma $\beta = 8\pi n_e kT/B^2$ is similar for both flares. It would not be surprising if both flares were the result of the same plasma processes: one event takes place in a large volume of the corona, the other flare is situated lower, in a denser and smaller region with a stronger magnetic field and exhibits a correspondingly shorter duration. The relationships between the parameters of the two flares are consistent with the relationships found from the statistical analysis in Paper 1. This shows that the two simple impulsive events of Sections 3 and 4 are exceptional with respect to their high intensity, but not with respect to their spectral and dynamical characteristics.

5. THE SOURCE OF AN ADIABATIC FLARE

5.1. Properties of a Single Temperature Plasma

The existence of single temperature plasmas during impulsive X-ray bursts indicates that temperature gradients must be nearly absent inside the source and very large in the transition layer at the border. The resulting physical picture for the hot flare source is a plasma confined by sharply defined walls with good heat insulation. The high mobility of energetic electrons explains the single temperature inside this bottle. On the other hand, strong magnetic fields must be responsible for the sharp confinement.

For the confining wall to resist the kinetic pressure $n_e kT$ of the hot bottle, the magnetic field strength B_w of the wall must be large enough that

$$\frac{B_w^2}{8\pi} \geqslant n_e kT$$

On the other hand, a single temperature inside the bottle indicates that the mobility of electrons is high not only along, but also across the field lines. If this were not the case the plasma could be divided in narrow tubes along the field lines. The slow drift of electrons perpendicular to the frozen-in magnetic fields would enable the plasma to have different temperatures in different tubes. The single temperature therefore means that the magnetic field strength B_i inside the bottle does not govern the particle motion. Thus we have the condition

$$\frac{B_i^2}{8\pi} \lesssim n_e kT,$$

corresponding to a high beta plasma, as deduced independently from the data.

5.2. Favorable Situation for Adiabatic Energy Transfer

The confinement of plasma as described in the previous section suppresses the most direct heat exchange mechanism, injection and ejection of large particle streams. Furthermore the heat conduction due to diffusion across the magnetic field lines of the walls is negligible during the impulsive flare phase; thus the situation is favorable for adiabatic energy transfer, in which there is no heat exchange with the environment. Other possible heat loss mechanisms are radiation and heat transfer due to wave energy passing through the wall of the bottle.

Radiation losses from plasmas at temperatures above 10 keV are primarily free-free emission and gyrosynchrotron radiation. According to Cap (1970) the total

gyrosynchrotron emission is larger than the total bremsstrahlung emission for temperatures higher than 6 keV; however, under solar conditions, the gyrosynchrotron radiation is almost completely reabsorbed by the source (see Fig. 6 of Drummond and Rosenbluth, 1963), and thus does not efficiently contribute to the heat exchange with the environment of the bottle. Only the free-free emission remains to be considered. For a thermal proton-electron plasma the radiative cooling time, t_{rad}, defined by

$$t_{rad} \doteq U_e \left(\frac{\partial U_e}{\partial t}\right)^{-1}_{ff}$$

follows from Tucker (1975). For T in units of keV and n_e in units of cm^{-3}

$$t_{rad} = 1.5 \cdot 10^{14} \frac{\sqrt{T}}{n_e} .$$

Using the temperature and density (K = 1) determined for the maximum phase of the 1970 March 1 flare yields $t_{rad} = 3 \cdot 10^6$ s. Even with much higher densities the radiation cooling time is longer than the duration of the impulsive flare phase. Therefore radiative energy loss can be neglected. The loss of the turbulent wave energy of the bottle is prevented by the steep gradients of temperature and magnetic field at the boundary of the hot plasma region. The abrupt change of physical parameters at this boundary is accompanied by jumps of the wave refractive indices resulting in reflection, rather than transmission, of the waves. Therefore the turbulent wave energy is trapped in the bottle also.

One additional requirement for adiabatic behavior does not follow from the picture of the single temperature bottle. The motion of the confining wall must be slow compared with the speed of the particles. The nonrelativistic energy gain of a particle with initial velocity v and mass m due to an elastic head-on collision with a wall of velocity v_w is given by

$$\Delta E = 2m(v\, v_w + v_w^2) .$$

For $v_w \ll v$, ΔE can be approximated by the term linear in v_w. This requirement is certainly fulfilled for electrons, since their typical speed at a coronal temperature of $2 \cdot 10^6$ K is already 10000 km s^{-1} and for temperatures of the hot flare sources it is 10 times larger.

For ions however the mean velocity is smaller so that in addition to the reversible term, an irreversible heating of ions takes place due to the influence of the v_w^2 term. This shows that the electron plasma undergoes a reversible change of state, whereas the total effect of the adiabatic compression and expansion is a net acceleration of ions.

5.3. On the Adiabatic Equation

Let us now consider the adiabatic equation for the relation between temperature and volume

$$T V^{\kappa - 1} = \text{constant}, \tag{8}$$

where κ is the adiabatic index. This equation can be written in terms of directly observable quantities, T and EM, because the confinement keeps the total number $N_e = n_e V$ of electrons constant. With $EM = N_e/V$ we get

$$\frac{T}{(EM)^{\kappa - 1}} = \text{constant}. \tag{9}$$

In a collision dominated plasma $\kappa = 5/3$. Because the relative change $\Delta E/E$ of the energy of individual particles depends only on the relative change $\Delta V/V$ of the volume (e.g. Fermi, 1966) a Maxwellian distribution remains Maxwellian all the time. Therefore the word "collision" does not necessarily mean interparticle collision, but any process which keeps the distribution isotropic. For example the interaction of whistler modes with electrons whose kinetic energy, E, is larger than the magnetic energy per electron, $B^2/8\pi n_e$, mainly serves to scatter the electrons without changing E (Kennel and Petschek, 1966). The above condition is fulfilled for the majority of electrons in a high beta plasma. The reflection of particles at the confining walls of the plasma also randomizes the velocity directions if the reflection properties are that of a rough surface.

Conversely, if there is no scattering at all, the two adiabatic invariants, magnetic moment and longitudinal invariant (e.g. Cap, 1970) are conserved. Then a change of the volume changes a Maxwellian to a bi-Maxwellian distribution function. The two temperatures $T_\parallel$ and $T_\perp$, parallel and perpendicular to the magnetic field, are independently determined by two adiabatic equations with two adiabatic indices $\kappa_\parallel$ and $\kappa_\perp$. For a compression parallel to the magnetic field $\kappa_\parallel = 3$ and $\kappa_\perp = 1$; for a compression perpendicular to the field (betatron acceleration) $\kappa_\parallel = 1$ and $\kappa_\perp = 2$; and if the geometry of the compression is isotropic the two equations reduce to the isotropic case with $\kappa_\parallel = \kappa_\perp = \kappa = 5/3$. The plasma can be described by the double-adiabatic magnetohydrodynamic theory (Cap, 1970). Thus it is not necessary to abandon the thermal model in a scatter-free situation.

ACKNOWLEDGMENTS

Many thanks are given to Prof. M. Waldmeier, Swiss Federal Observatory and Dr. G. Olivieri, Paris Observatory for sending us Hα heliograms, to Dr. H. Urbarz, University of Tübingen for the radio spectrogram and to Dr. A. Magun, University of Bern for the 10.5 GHz burst plot with high time resolution.

We sincerely thank Judy Karpen for critical reading of this manuscript.

In carrying out this research the authors have benefited considerably from their participation in the Skylab Solar Workshop Series on Solar Flares. The Workshops are sponsored by NASA and NSF and managed by the High Altitude Observatory, National Center for Atmospheric Research.

This research was done while one of the authors (C. M.) was a visiting scientist at the Laboratory for High Energy Astrophysics of the NASA Goddard Space Flight Center with a Fellowship from the Swiss National Science Foundation. The hospitality of Drs. F. B. McDonald and R. Ramaty is gratefully acknowledged.

REFERENCES

Bai, T. and Ramaty, R.: 1977, to be published in Astrophys. J.

Benz, A. O. and Gold, T.: 1971, Solar Phys. 21, 157.

Bowen, P. Y., Norman, K., Pounds, K. A., Sanford, P. W. and Willmore, A. P.: 1964, Proc. Roy. Soc. 281, 538.

Brown, J. C. and Hoyng, P.: 1975, Astrophys. J. 200, 734.

Cap, F.: 1970, "Einführung in die Plasmaphysik I", Vieweg + Sohn, Braunschweig, p. 70, p. 192.

Chubb, T. A.: 1970, in Dryer (ed.) "Solar Terrestrial Physics I: Part I," D. Reidel Publ. Co., Dordrecht, Holland, p. 99.

Cranneil, C. J., Frost, K. J., Mätzler, C., Ohki, K. and Saba, J. L.: 1977, to be published (Paper 1).

Drummond, W. E. and Rosenbluth, M. N.: 1963, Phys. Fluids 6, 276.

Fermi, E.: 1966, "Notes on Thermodynamics and Statistics," The University of Chicago Press, Chicago, p. 13.

Frost, K. J.: 1969, Astrophys. J. 158, L159.

Hoyng, P.: 1975, Thesis, University of Utrecht.

Kahler, S.: 1971, Astrophys. J. 164, 365.

Kahler, S.: 1975, in Kane, S. R. (ed.) "Solar Gamma, X- and EUV Radiation," IAU Symposium No. 68, 211.

Kane, S. R. and Anderson, K. A.: 1970, Astrophys. J. 162, 1003.

Kennel, C. F. and Petschek, H. E.: 1966, J. Geophys. Res. 71, 1.

Koch, H. W. and Motz, J. W.: 1959, Rev. Mod. Phys. 31, 920.

Langer, S. H. and Petrosian, V.: 1977, Astrophys. J. 215, 666.

Ramaty, R.: 1969, Astrophys. J. 158, 753.

Santangelo, N., Horstman, H. and Horstman-Moretti, E.: 1973, Solar Phys. 29, 143.

Spicer, D. S.: 1976, NRL Report 8036, Naval Research Lab., Washington, D. C.

Spitzer, L.: 1962, "Physics of Fully Ionized Gases," New York, Interscience Publishers.

Tomblin, F. F.: 1972, Astrophys. J. 171, 377.

Tucker, W. H.: 1975, "Radiation Processes in Astrophysics," MIT Press, Cambridge, Mass.